

STARS

University of Central Florida
STARS

Faculty Bibliography 2010s

Faculty Bibliography

1-1-2013

Imaging of Benign Soft Tissue Tumors

Laura W. Bancroft
University of Central Florida

Christopher Pettis
University of Central Florida

Christopher Wasyliw

Find similar works at: <https://stars.library.ucf.edu/facultybib2010>

University of Central Florida Libraries <http://library.ucf.edu>

This Article is brought to you for free and open access by the Faculty Bibliography at STARS. It has been accepted for inclusion in Faculty Bibliography 2010s by an authorized administrator of STARS. For more information, please contact STARS@ucf.edu.

Recommended Citation

Bancroft, Laura W.; Pettis, Christopher; and Wasyliw, Christopher, "Imaging of Benign Soft Tissue Tumors" (2013). *Faculty Bibliography 2010s*. 3657.

<https://stars.library.ucf.edu/facultybib2010/3657>



Imaging of Benign Soft Tissue Tumors

Laura W. Bancroft, MD^{1,2,3} Christopher Pettis, MD^{1,2} Christopher Wasyliw, MD^{1,2}

¹Department of Radiology, Florida Hospital

²University of Central Florida School of Medicine, Orlando, Florida

³Florida State University School of Medicine, Tallahassee, Florida

Address for correspondence Laura W. Bancroft, MD, Florida Hospital, 601 E. Rollins, Orlando, FL 32803 (e-mail: Laura.Bancroft.md@flhosp.org).

Semin Musculoskelet Radiol 2013;17:156–167.

Abstract

The evaluation of soft tissue tumors should be approached systematically, with careful assessment of the patient's age, clinical presentation, anatomical location of the mass, and MRI characteristics. The imaging evaluation of a suspected soft tissue mass begins with conventional radiography to exclude an underlying osseous lesion and assess for any lesional calcification. MRI is particularly useful in evaluating the signal intensity, enhancement pattern, and extent of soft tissue masses that can expand beyond fascial planes and involve the neurovascular bundle, joint, or bone. Among the common benign soft tissue tumors, a fairly definitive imaging diagnosis can be made in cases of lipoma, elastofibroma dorsi, hemangiomas, myositis ossificans, giant cell tumor of tendon sheath, and peripheral nerve sheath tumors. In the remaining cases, the differential diagnosis can be narrowed by knowing the patient's demographics and any associated syndromes, in conjunction with recognizing specific MRI features. Knowledge of the World Health Organization's tumor designations and the incidence of specific tumors based on patient age and anatomical location are vital tools for the interpreting radiologist.

Keywords

- ▶ MRI
- ▶ benign
- ▶ soft tissue
- ▶ tumor

The evaluation of soft tissue tumors should be approached systematically, with careful assessment of the patient's age, clinical presentation, anatomical location of the mass, presence or absence of calcification, and MRI characteristics.^{1–3} The imaging evaluation of a suspected soft tissue mass begins with conventional radiography, which serves to exclude an underlying osseous lesion and evaluate for the presence or absence of mineralization. MRI is particularly useful in evaluating the signal intensity, enhancement pattern, and extent of soft tissue masses that can expand beyond fascial planes and involve the neurovascular bundle, joint, or bone.^{1,4}

MRI protocols for the evaluation of tumors must be performed in at least two orthogonal planes and include T1-weighted and T2-weighted sequences. Additional sequences to consider include gradient-echo imaging for the detection of hemorrhage, T1-weighted fat-suppressed images to differentiate fat from hemorrhage, and enhanced imaging after contrast administration.^{1–5} Several benign soft tissue tumors can be diagnosed fairly definitively with imaging, whereas the differential diagnosis of indeterminate lesion

can be narrowed significantly by combining knowledge of the MRI signal characteristics and the incidence of specific tumors based on patient age and anatomical location.^{1,6,7} Although it is reassuring to know that benign soft tissue lesions outnumber malignant tumors by a factor of 100:1, masses deemed indeterminate by imaging criteria are often referred for definitive biopsy.⁵ This imaging pictorial reviews the more common benign soft tissue tumors of the musculoskeletal system among each of the histologic categories, as outlined by the World Health Organization (WHO).⁸

Adipocytic Tumors

Adipocytic tumors represent the largest single group of mesenchymal tumors, and benign subtypes include lipoma, lipomatosis, lipomatosis of nerve, lipoblastoma/lipoblastomatosis, angiolipoma, myolipoma of soft tissue, chondroid lipoma, spindle cell lipoma/pleomorphic lipoma, and hibernoma.⁹ Benign lipomatous lesions represent a vast array of tumors that demonstrate a predominance of adipose signal

Issue Theme Current Developments and Recent Advances in Musculoskeletal Tumor Imaging; Guest Editor, Jeffrey James Peterson, MD.

Copyright © 2013 by Thieme Medical Publishers, Inc., 333 Seventh Avenue, New York, NY 10001, USA.
Tel: +1(212) 584-4662.

DOI <http://dx.doi.org/10.1055/s-0033-1343071>.
ISSN 1089-7860.

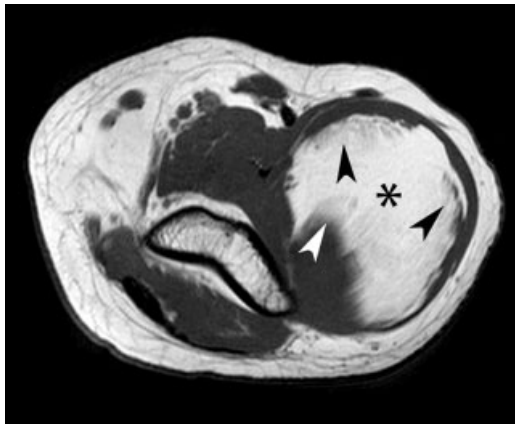


Fig. 1 Intramuscular lipoma in brachialis. Axial T1-weighted image shows a fatty mass (asterisk) in the brachialis that is isointense to subcutaneous fat. Notice the ill-defined margins (arrowheads) due to the pliable fat infiltrating among the muscular fibers.

on MRI; however, specific imaging features of various subtypes are beyond the scope of this article and may be referenced more thoroughly in the literature.^{11–15} Furthermore, MRI may not always allow differentiation of benign and malignant fatty tumors, but lesions >10 cm, thick septa, and globular and/or nodular nonadipose areas should raise concern for liposarcoma.¹²

Lipoma is the most common benign soft tissue tumor, is composed of mature adipocytes, and most commonly presents as a slow-growing palpable mass in middle-age patients.¹⁰ Lipomas are often not imaged but follow fat on all image sequences. It has been estimated that 70 to 90% of adipocytic tumors have a diagnostic imaging appearance.¹ Superficial lipomas can blend imperceptibly with the surrounding subcutaneous fat, whereas intramuscular lipomas can have ill-defined margins due to fat infiltration among muscle fibers in deep-seated lesions (►**Fig. 1**). Intramuscular lipomas occur most often in the thigh, shoulder, and upper arm, and they are most common in men between the ages of 30 and 60.¹⁶

Lipomatosis (also known as Madelung disease) is a rare diffuse overgrowth of mature adipocyte in the subcutis and muscles that occurs in children <2 years of age or in adults.¹⁷ Diffuse lipomatosis usually involves the trunk but can involve most of an extremity, head and neck, abdomen, and pelvis.¹⁷ When extremities are involved, the distal portions of the forearms and legs are unaffected.¹⁶ It can also be associated with macrodactyly, although there is no involvement of the nerve as with neural fibrolipoma.¹⁶ MRI demonstrates hyperintense T1-weighted fat within and between the involved muscles and/or the subcutaneous tissues (►**Fig. 2**).^{18,19}

The diagnosis of lipoblastoma and lipoblastomatosis should always be high on the differential diagnosis list when a fatty mass is identified in a young child. Lipoblastoma

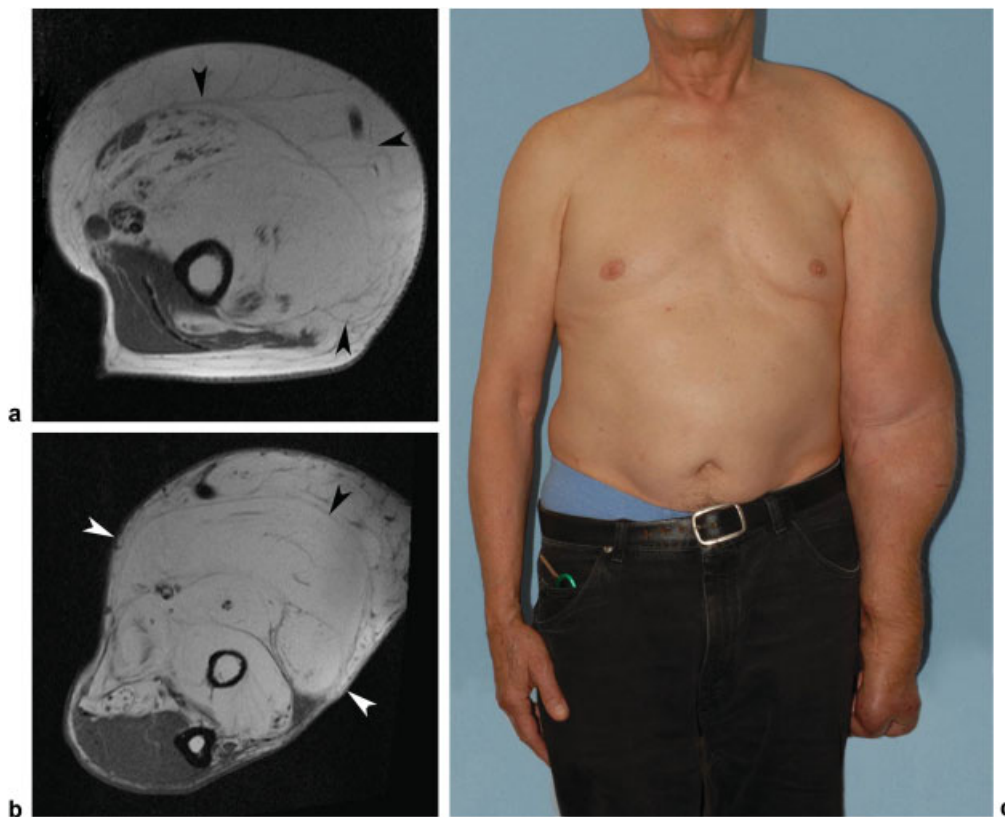


Fig. 2 Lipomatosis of left arm. (a, b) Axial T1-weighted images of the left arm (a) and forearm (b) demonstrate marked subcutis and muscular lipomatous infiltration (arrowheads) of the anterior compartment of the arm and extensor compartment of the forearm. No thickened septa or nodular nonadipose components are present. (c) Clinical photograph shows diffuse enlargement of the left upper extremity.

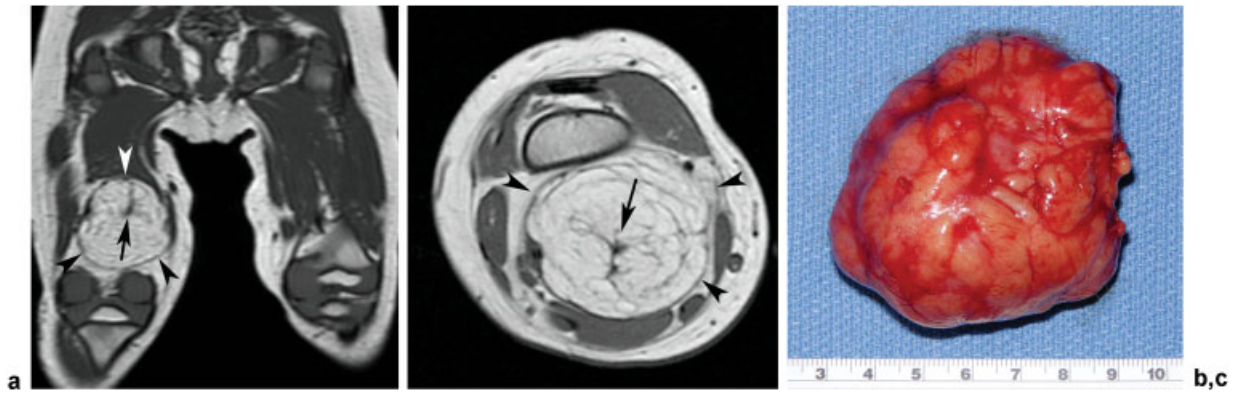


Fig. 3 Lipoblastoma of thigh of a 3-month-old boy. (a, b) Coronal (a) and axial (b) images through the right thigh show a well-circumscribed fatty mass (arrowheads) in the posterior compartment with multiple septations, some of which are confluent (arrow). No nodular nonadipose components are present. (c) Resected specimen shows the corresponding well-circumscribed fatty mass that proved to be lipoblastoma.

and lipoblastomatosis refer to the circumscribed and diffuse forms of the same tumor.¹⁶ Lipoblastoma is a localized tumor composed of cells resembling fetal adipose tissue, and it is most commonly detected as a palpable mass in a child <3 years of age, with boys affected two to three times more frequently than girls.^{14–16} Lipoblastoma is a slow-growing, well-circumscribed mass that most commonly involves the extremities but can affect the mediastinum, retroperitoneum, trunk, head, and neck.¹⁴ On MRI, lipoblastoma is a well-circumscribed mass that is predominantly fatty, but non-lipomatous areas may have a nonspecific appearance and may simulate liposarcoma.¹⁰ MR imaging of lipoblastoma has been reported as relatively hypointense to subcutaneous fat on T1-weighted imaging and containing thin septae. Lesions may demonstrate cystic change and display variable enhancement patterns ranging from none, to mild, to marked and heterogeneous (–Fig. 3).^{13,15} Lipoblastomatosis is the corresponding unencapsulated diffuse process in which the subcutis and underlying muscle of young children are invaded by these fatty masses.¹⁶

Fibroblastic/Myoblastic Tumors

The numerous benign fibroblastic/myofibroblastic tumors include desmoid-type fibromatosis, elastofibroma, myositis ossificans, myofibroma and fibro-osseous pseudotumor of digits, nodular fasciitis, proliferative fasciitis, and ischemic fasciitis, among others.²⁰ For simplification, the musculoskeletal fibromatoses have been subdivided into superficial (fascial) and deep (musculoaponeurotic) groups.²⁰ The superficial fibromatoses (palmar fibromatosis, plantar fibromatosis, juvenile aponeurotic fibroma, and infantile digital fibromatosis) are small slow-growing tumors, whereas the deep musculoskeletal tumors (infantile myofibromatosis, fibromatosis colli, extra-abdominal desmoids tumor, and aggressive infantile fibromatosis) are typically large, rapidly growing, and aggressive.^{20–22} Desmoid-type fibromatosis is an infiltrative clonal fibroblastic proliferation that arises in deep connective tissue in muscle, fascia, or aponeuroses of patients between the teenage years and 40 years of age.^{22,23} Extra-abdominal fibromatosis often involves the shoulder, chest wall, back, thigh, head and neck, and knee.^{20,21} An

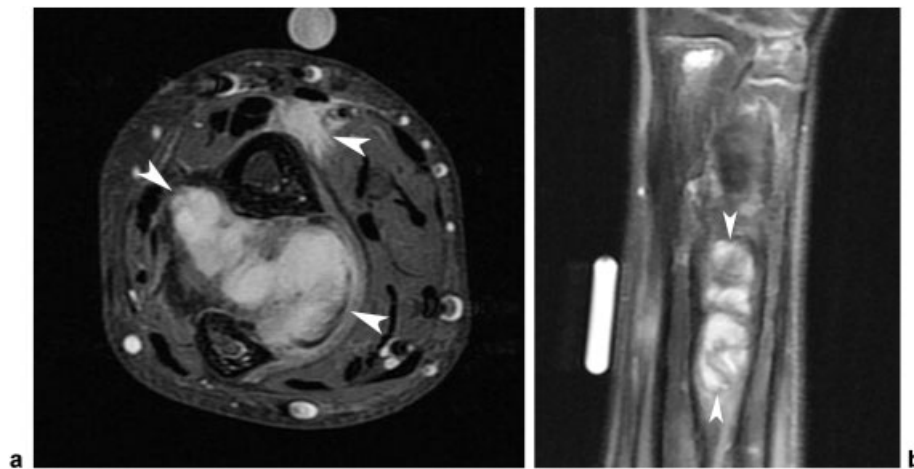


Fig. 4 Desmoid-type fibromatosis of forearm in a 15-year-old boy. (a, b) Axial (a) and sagittal (b) fast spin-echo T1-weighted enhanced fat-suppressed images depict marked heterogeneous enhancement of the soft tissue masses (arrowheads) extending into the distal interosseous space and lateral to the radius. No osseous erosion or invasion is identified.

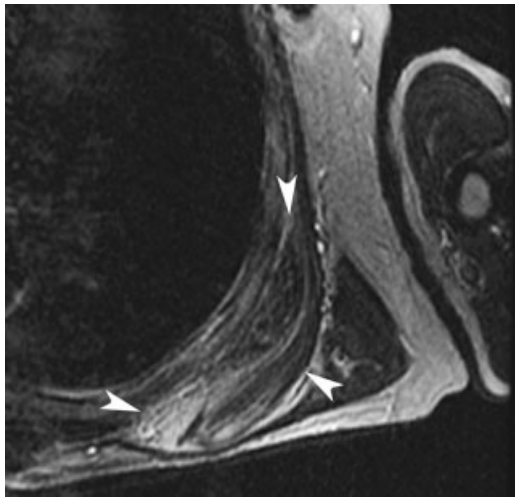


Fig. 5 Elastofibroma about left inferior scapula. Axial T2-weighted image shows classic location of elastofibroma (arrowheads) about the inferior pole of the scapula, deep to the serratus anterior muscle. The elastofibroma is primarily isointense relative to skeletal muscle, with interlaced streaks of adipose tissue.

estimated 50 to 70% of fibromatoses have a diagnostic imaging appearance on imaging; thus biopsy is usually required except for lesions in the superficial hands or feet.¹ Desmoids are homogeneously isointense to skeletal muscle on T1-weighted images, heterogeneously hyperintense on T2-weighted images, and demonstrate marked enhancement of the noncollagenase components (►Fig. 4).²⁴ Hypointense bands likely correspond to dense conglomerations of collagen bundles and do not enhance.^{25,26} MRI is particularly useful in determining if lesions are single or multiple (multiple in 15% of cases), delineating the extent of these infiltrative lesions, depicting any neurovascular encasement, and evaluating for response to treatment.^{20,27}

Elastofibroma dorsi is an ill-defined slow-growing fibroelastic tumorlike lesion classified by the WHO as a benign fibroblastic/myofibroblastic tumor. Elastofibroma likely rep-

resents a response to repeated trauma or friction, most often occurs in the soft tissues between the inferior scapula and chest wall in up to 13 to 17% of elderly individuals (more commonly in women), and is often bilateral.²⁸⁻³¹ Less commonly, elastofibroma may occur overlying the elbow or ischial tuberosity, deltoid muscle, foot, or visceral locations.³⁰ Although lesions are often incidentally detected during computed tomography (CT) of the chest performed for other reasons, MRI can be performed for patients presenting with growing, painful, or “snapping” periscapular masses, and MR is typically diagnostic in cases of elastofibroma dorsi. Lesions typically demonstrate a mass at the inferior pole of the scapula that is most often deep to the serratus anterior and latissimus dorsi, and isointense relative to skeletal muscle interlaced with streaks of adipose tissue (►Fig. 5).^{29,31}

Myositis ossificans (MO) is subcategorized into posttraumatic and nontraumatic/pseudomalignant forms and myositis ossificans progressiva.³² Posttraumatic myositis ossificans is the most common form (occurring in ~75% of cases) and usually seen more commonly in men in the second and third decades.³³ MO is a localized self-limiting reparative lesion composed of reactive fibrous tissue and bone) that can be the result of a direct blow.^{32,34} Lesions most commonly affect the vastus lateralis, brachialis, intercostals spaces, erector spinae, pectoralis, gastrocnemius, and gluteal muscles.³³ The three phases of MO are the acute (pseudoinflammatory), subacute (pseudotumoral), and chronic (self-limited) phases.³⁵ CT is the imaging modality of choice because it best demonstrates the zonal pattern of calcification expected at the various phases of development. CT demonstrates nonspecific soft tissue swelling in the first few weeks, but a characteristic peripheral calcified rim of variable thickness and central isodensity develops after several weeks, and that rim becomes denser and more confluent on subsequent imaging (►Fig. 6).³⁴ It is estimated that >95% of cases of MO have a diagnostic imaging appearance on imaging.¹

The MRI appearance of MO also depends on the stage of maturation. The initial MRI findings of MO show striking

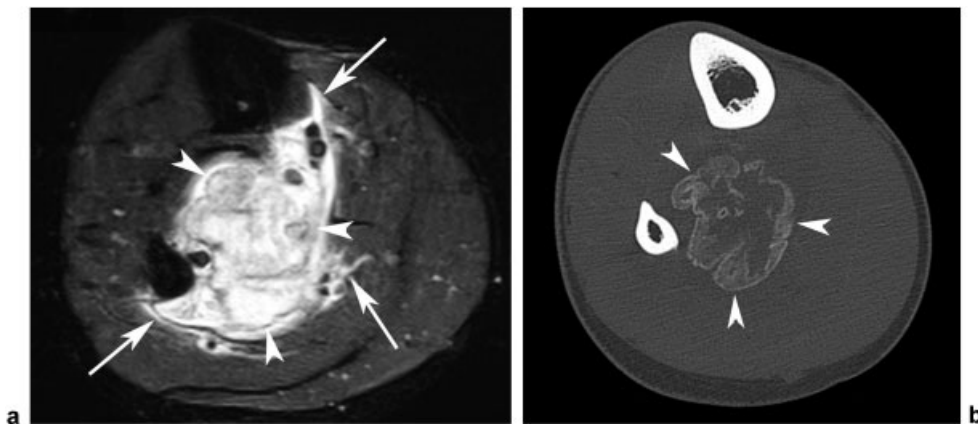


Fig. 6 Myositis ossificans in a 23-year-old man with an 8-week history of calf pain. (a) Axial fast spin-echo T2-weighted image of the right calf shows edema-like signal changes (arrows) surrounding a heterogeneously hyperintense soft tissue mass (arrowheads) in the deep compartment of the midcalf. (b) Corresponding nonenhanced computed tomography shows a peripherally calcified mass (arrowheads), diagnostic of evolving myositis ossificans. Mass was not biopsied, and patient was conservatively managed and followed.

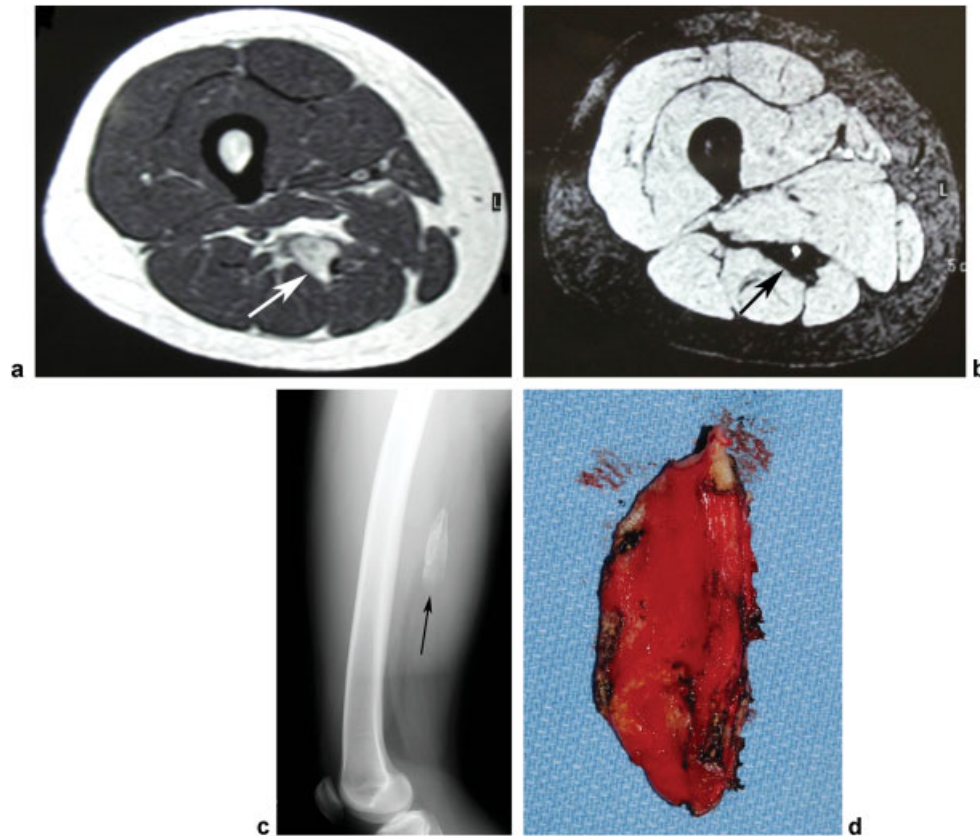


Fig. 7 Mature myositis ossificans. (a, b) Axial proton-density (a) and T2-weighted fat-suppressed (b) images through the right midthigh of a 17-year-old girl with a 5-year history of thigh pain demonstrate a well-circumscribed mass (arrow) in the posterior compartment of the thigh with hypointense margin and internal signal that is isointense to marrow. No associated edema-like signal changes are evident. (c) Lateral radiograph confirms mature heterotopic ossification. Due to complaint of pain with resisted knee flexion, patient was taken to surgery. (d) Photograph of the resected specimen, which was confirmed myositis ossificans.

heterogeneous edema-like signal changes within the enlarged muscle. Next, a masslike hyperintense T2-weighted signal focus develops within the surrounding edema-like signal changes during the first days to 1 week after the trauma (►Fig. 6). MRI often shows a well-defined mass with peripheral low signal within maturing MO, corresponding to peripheral mineralization (►Fig. 7).³⁵ MO may be confused with parosteal or soft tissue osteosarcoma; however, sarcomas develop over a longer period of time than MO and typically do not have the intense surrounding edema-like signal changes characteristic of the acute and subacute phases.

Fibrohistiocytic Tumors

Giant cell tumor of tendon sheath (GCTTS), diffuse-type GCT, deep benign fibrous histiocytoma, plexiform fibrohistiocytic tumor, and giant cell tumor of soft tissue are all benign fibrohistiocytic tumors.³⁶ Of these lesions, GCTTS is the most common. This is the focal form of pigmented villonodular synovitis, which presents in patients between 30 and 50 years of age, more commonly in women.³⁶ GCTTS occurs most often in the hand and fingers along the synovium of the tendon sheath or interphalangeal joint, followed by the wrist, ankle/foot, and knee.³⁶ T1-weighted imaging typically shows

mixed intermediate to low signal intensity soft tissue nodule, low signal intensity on fluid-sensitive sequences, and characteristic “blooming” (further signal loss) if gradient-echo imaging is acquired (►Figs. 8 and 9). Lesions can be fairly reliably differentiated from fibroma of tendon sheath on MRI because fibroma will be intermediate to low signal intensity on T2-weighted images and not “bloom” on gradient-echo imaging.³⁷ An estimated 70 to 90% of cases of GCTTS have a diagnostic imaging appearance on imaging, and lesions are often resected without biopsy.¹

Smooth Muscle Tumors

Angioleiomyoma (also known as angiomyoma) and leiomyoma of deep soft tissue are the two benign smooth muscle tumors.³⁸ Angioleiomyoma is a small (<2 cm) vascular smooth muscle tumor that arises from the tunica media of veins or arteries. These tumors occur most often in women in their fourth to sixth decades, and they present as painful, slow-growing masses in which pain may be exacerbated by cold, wind, pressure, pregnancy, or menses.³⁹ MRI typically demonstrates a well-defined oval mass located superficial to the fascia with the most common sites the hand, ankle and foot, and knee.^{39–41} In a series of 10 cases, angioleiomyoma was solitary and most commonly isointense to muscle on T1-

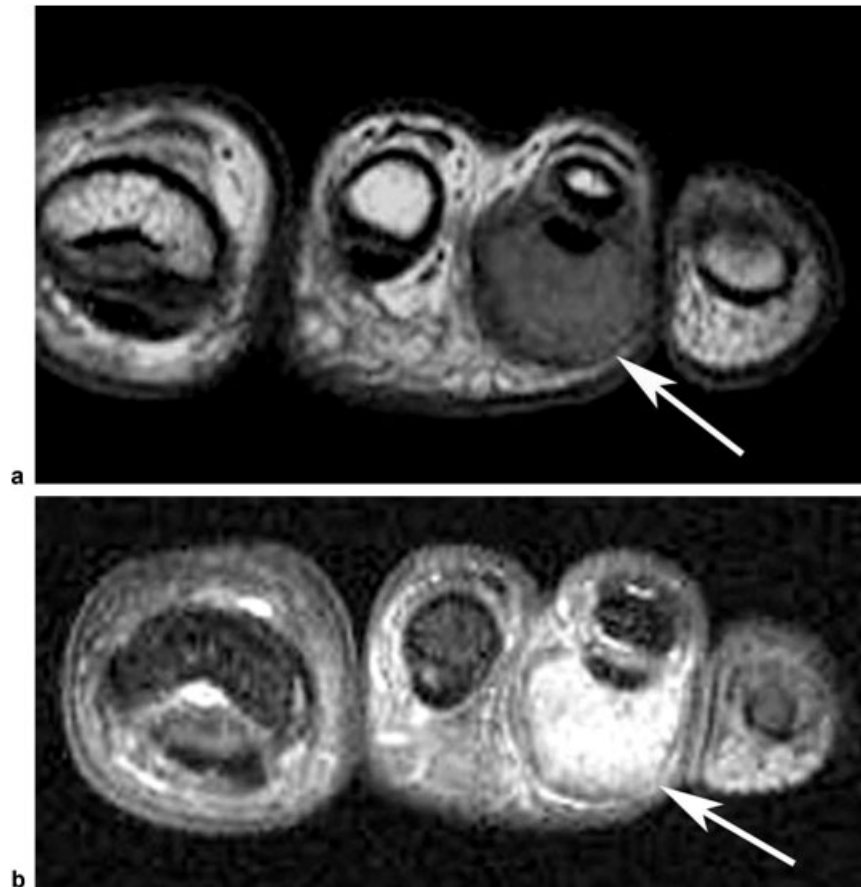


Fig. 8 Giant cell tumor of tendon sheath. (a, b) Axial proton density (a) and T1-weighted enhanced fat-suppressed (b) images show a well-circumscribed nodule (arrows) extending along the flexor tendon sheath of the third toe that is nearly isointense to skeletal muscle and markedly enhances.

weighted images, heterogeneously hyperintense on fluid-sensitive sequences (with multiple linear or branching areas of hyperintensity), and diffusely or heterogeneously enhanced.⁴²

Leiomyoma of deep soft tissue is exceptionally rare, with a mean age of 25 years at presentation, occurring equally in

men and women.⁴³ Whereas angioleiomyoma is confined to the subcutaneous or dermal regions, the leiomyoma of deep soft tissue can arise in the deep somatic soft tissue (most commonly the extremities), retroperitoneum, or abdominal cavity.⁴³ Tumors are well-circumscribed, frequently calcified masses, with “mulberry-like” or extensive calcification on

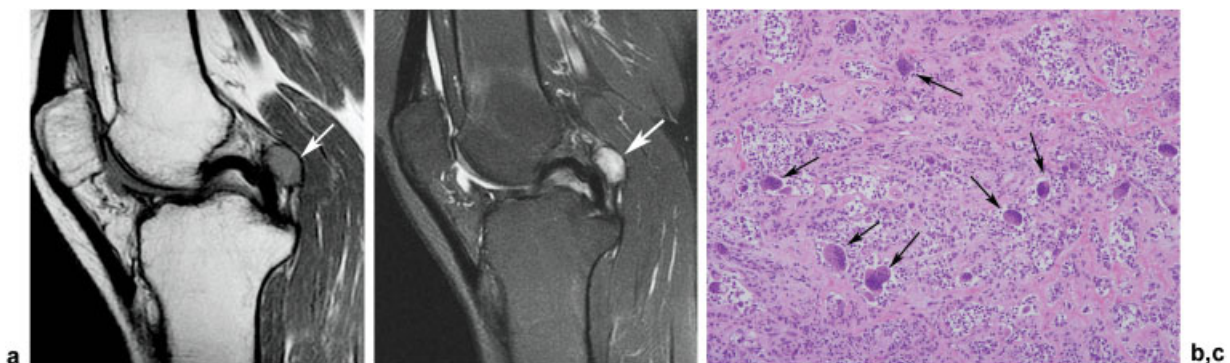


Fig. 9 Focal pigmented villonodular synovitis of posterior knee joint in a 41-year-old woman with knee pain. (a, b) Sagittal fast spin-echo proton density (a) and T2-weighted fat-suppressed images delineate a well-circumscribed soft tissue nodule (arrows) located between the posterior joint capsule and posterior cruciate ligament. Nodule is heterogeneously hyperintense on T2-weighted image, with foci of intermediate and low signal. Patient was treated with open posterior excision and synovectomy. (c) Microscopic section shows admixture of histiocytoid cells, foamy cells, lymphocytes, and giant cells (arrows) (hematoxylin and eosin).

radiographs or CT.⁴⁴ Reported MR imaging characteristics include a well-circumscribed mass that is isointense to skeletal muscle on T1-weighted images, isointense to slightly hyperintense on T2-weighted images, contains punctuate signal voids corresponding to calcification, prominent vascular channels, and homogeneously enhanced (except for the regions of calcification) due to their marked vascularity.^{44,45}

Pericytic (Vascular) Tumors

Glomus tumor and myopericytoma are the two pericytic tumors classified by the WHO.⁴⁶ Glomus tumor is a rare mesenchymal tumor that histologically resembles modified smooth muscle cells of the glomus body. It occurs in both the adult and pediatric population, with a mean tumor size of ~1 cm.⁴⁷ Patients almost always present with prolonged history of focal and often debilitating pain, and most glomus tumors occur in the distal hand (75%) or foot, especially in the subungual region (65%).^{46,47} Glomus tumors are well-circumscribed nodules that are intermediate to skeletal muscle on T1-weighted images, hyperintense on T2-weighted imaging, and demonstrate marked homogeneous enhancement when <1 cm. Larger lesions can be lobulated and demonstrate T2 heterogeneity and heterogeneous enhancement.⁴⁷ Osseous erosion is observed in 22 to 82% of nail bed glomus tumors.⁴⁸

Skeletal Muscle Tumors

Rhabdomyoma is the only benign mesenchymal tumor with skeletal muscle differentiation and much more rare than the malignant counterpart, rhabdomyosarcoma, occurring in <2% of all striated muscle tumors.³⁹ Rhabdomyoma is categorized into either cardiac or extracardiac subtypes. The cardiac subtype is associated with tuberous sclerosis, whereas the extracardiac subtype is very rare and not associated with this syndrome.^{39,49} Extracardiac rhabdomyoma is classified as adult, fetal, or genital, and it has a predilection for the head and neck. The adult type of rhabdomyoma typically

presents as a solitary nonpainful mass in adults with a median age of 60 years, more commonly in men.⁵⁰ MR imaging reports in the literature are sparse but report a well-defined mass that is isointense or hyperintense to skeletal muscle on T1- and T2-weighted images, may contain central hemorrhagic necrosis, and either homogeneously or heterogeneously enhance.^{50,51}

Vascular Tumors

Vascular lesions have several different classification systems, depending on the perspective of the clinician, pathologist, or radiologist. Benign nonaggressive vascular lesions are categorized by the WHO as hemangioma, epithelioid hemangioma, angiomas, and lymphangioma.⁵² Lesions are often divided from the radiologist's perspective into "low-flow" (lymphatic and venous malformations) and "high-flow" (arteriovenous malformations) vascular malformations for diagnostic and therapeutic purposes.⁵³ Hemangioma is one of the most common soft tissue tumors, and it is subcategorized into capillary, cavernous, venous, and arteriovenous varieties, among others.⁵⁴

Intramuscular hemangioma (angioma) is a deep hemangioma, in which there is a proliferation of benign vascular channels within skeletal muscle associated with a variable amount of fatty tissue.⁵² Lesions most commonly occur in young adults and affect men and women equally. Most often lesions involve the thigh, head and neck, arm, and trunk.⁵⁴ An estimated 90 to 95% of hemangiomas have an imaging appearance that is diagnostic.¹ Lesions are typically isointense or hypointense to muscle on T1-weighted imaging, demonstrate areas of intralesional fat, and are heterogeneously hyperintense on T2-weighted images. Lesions often contain tubular vessels primarily aligned in a parallel orientation and can contain signal voids corresponding to phleboliths (▶ Fig. 10).⁵⁴

Venous hemangioma is composed of veins of variable size and mainly presents in adults. Venous hemangiomas have

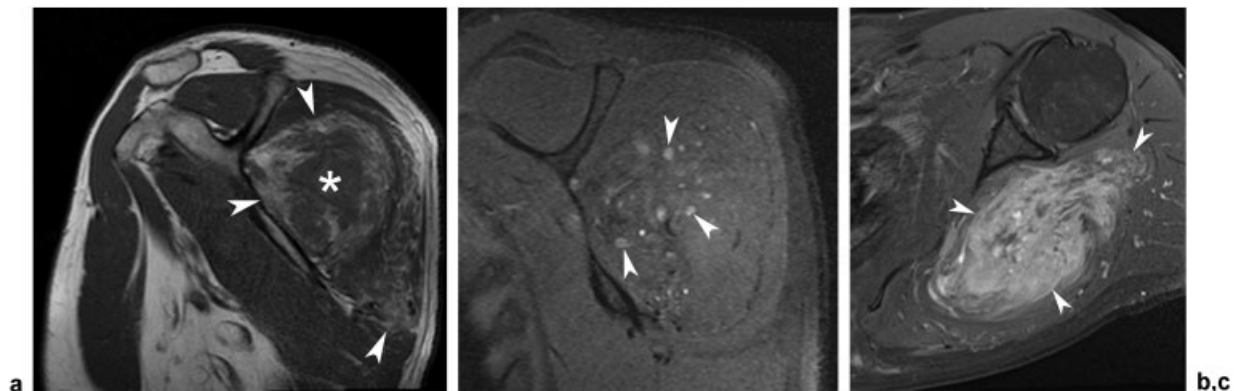


Fig. 10 Hemangioma of infraspinatus and teres minor muscles. (a) Sagittal T1-weighted image shows a heterogeneous soft tissue mass (asterisk) throughout the infraspinatus and teres minor muscles with predominantly peripheral fatty replacement of the musculature (arrowheads). Fatty muscular atrophy is secondary to vascular shunting by the hemangioma. (b) Sagittal T1-weighted fat-suppressed (FS) image obtained before contrast administration depicts multiple hyperintense (arrowheads) and hypointense ovoid signal foci corresponding to thrombosed vessels seen in cross section. (c) Axial T1-weighted enhanced FS image delineates the extent of the mass (arrowheads) that contains multiple enhancing tubular structures primarily aligned in a parallel orientation.

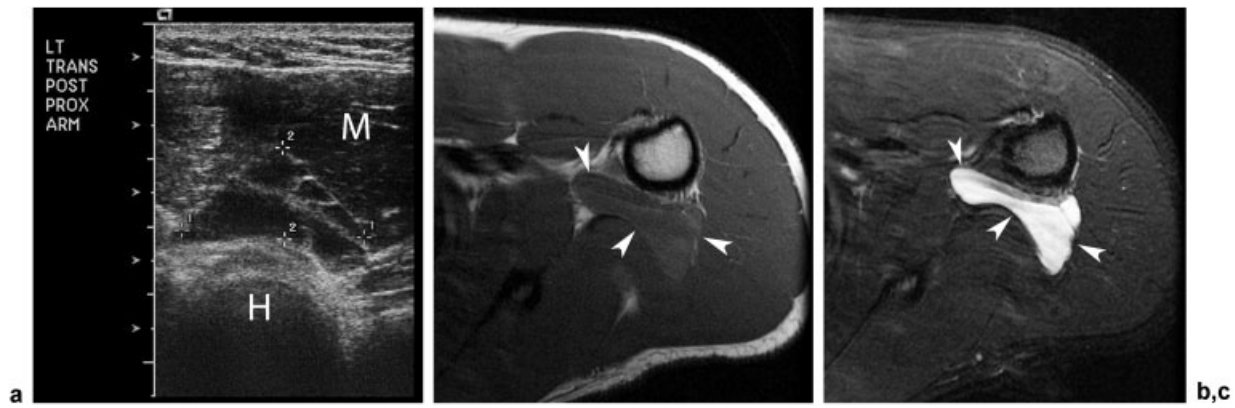


Fig. 11 Lymphangioma in a 16-year-old boy with aching shoulder. (a) Transverse sonograph obtained from posterior approach shows a multiloculated macrocystic lesion that insinuates between the deltoid and triceps muscles (M) and the humerus (H). (b, c) Axial images show a multiloculated cystic structure (arrowheads) in the quadrilateral space that is slightly hyperintense to muscle on T1-weighted sequence (a) and markedly hyperintense on T2-weighted fat-suppressed image (b). Lesion was resected and proved to be lymphangioma.

large thick-walled veins that often thrombose and form phleboliths. Arteriovenous hemangioma (malformation) is a nonneoplastic vascular lesion with arteriovenous shunts that can be either deep seated or cutaneous.⁵² Lesions demonstrate hypertrophied arteries and dilated venous spaces as low-signal tubular structures on T1- and T2-weighted images. Magnetic resonance angiography with contrast enhancement can often better define the feeding arteries and draining veins.⁵⁵

Large vascular lesions with high degree of shunting can lead to limb hypertrophy and heart failure. In addition, giant cavernous hemangiomas can be complicated by thrombocytopenic purpura, in which the tumors sequester platelets, leading to consumption coagulopathy (Kasabach-Merritt syndrome).^{52,54,56} Multiple other syndromes involving hemangiomas exist including Maffucci syndrome, a rare mesodermal dysplasia in which multiple hemangiomas and enchondromas are present. With Maffucci syndrome there

is a 20 to 30% incidence of malignant tumors developing (mainly chondrosarcoma).⁵⁷

Lymphangioma is a benign cavernous or cystic vascular lesion composed of dilated lymphatic channels containing watery or milky fluid.⁵⁸ Lesions are common in the pediatric population, and most present at birth or during the first years of life with focal painless swelling.^{58,59} Cystic lymphangioma most often involves the head and neck (48%), axilla, and groin; the cavernous type also occurs in the upper trunk, extremities, and abdomen.^{53,58} Lesions that contain cystic spaces >2 cm are termed *macrocytic lymphatic malformations*, and those with cystic foci <2 cm are termed *microcystic*.⁵³ Lesions can rapidly enlarge due to hemorrhage or infection.⁵³ On sonography, lymphangioma is evident as a cystic lesion with multiple septations of varying thickness and occasional fluid-fluid levels due to prior hemorrhage (►Fig. 11a).⁵⁹ Macrocytic lymphangioma characteristically presents as a heterogeneous fluid-filled mass on MRI that is isointense to muscle on

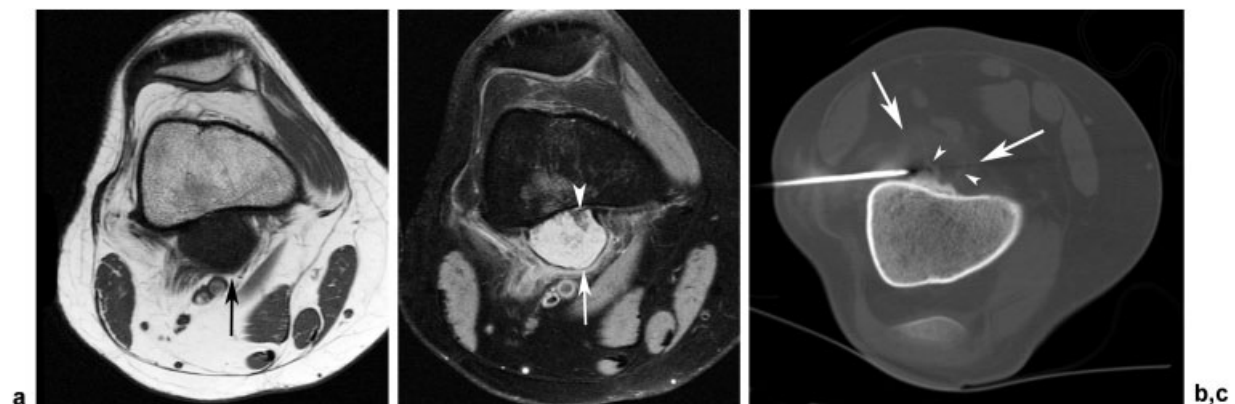


Fig. 12 Juxtacortical chondroma in a 19-year-old woman with intermittent knee pain. (a, b) Axial imaging of the distal femoral metadiaphysis shows a well-circumscribed mass (arrow) abutting the femoral cortex that is hypointense to muscle on T1-weighted image (a) and hyperintense with areas of low signal (arrowhead) on T2-weighted image (b). (c) Computed tomography-guided biopsy of the mass (arrowheads) from lateral approach demonstrated this to be a periosteal chondroma. Note the internal mineralization (arrows), most marked along the posterior aspect of the mass. Intralesional excision was subsequently performed.

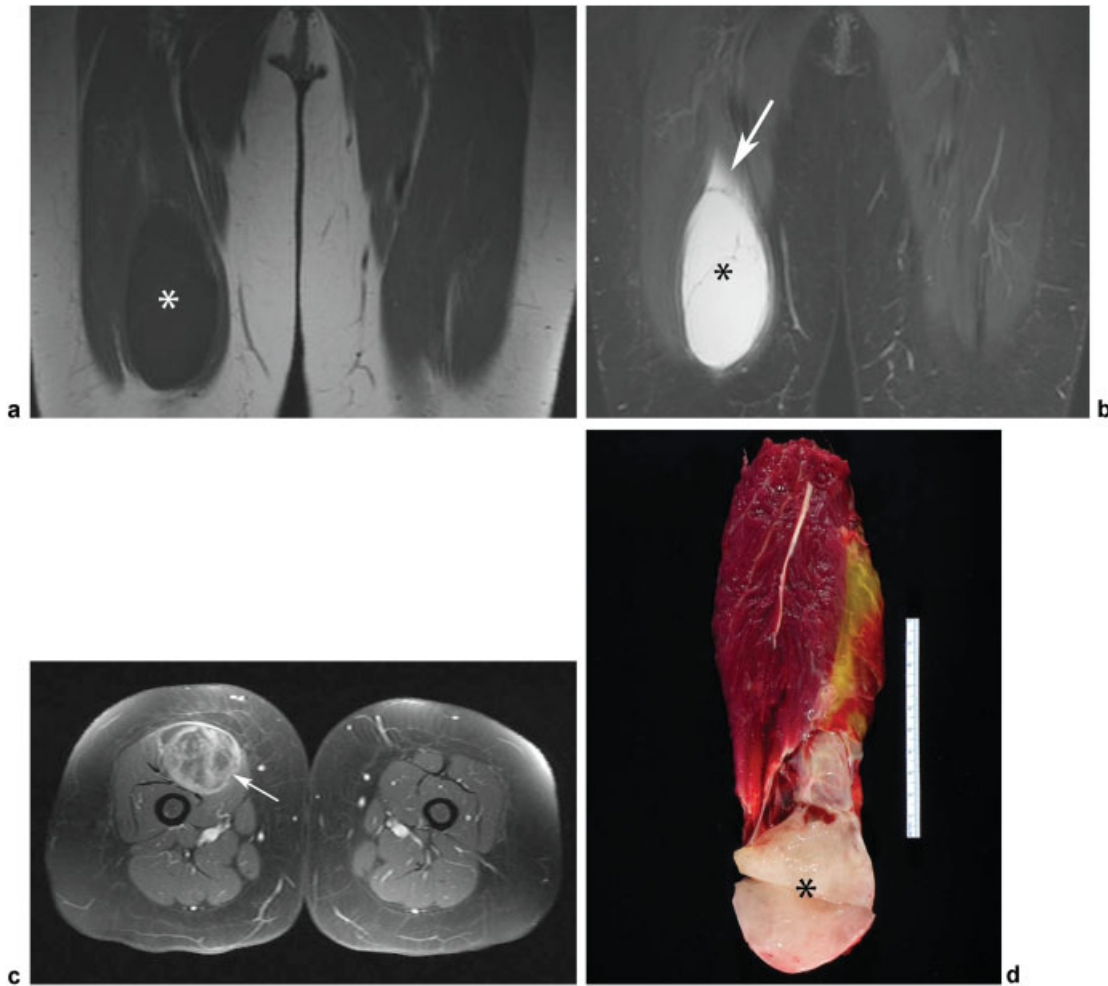


Fig. 13 Intramuscular myxoma of right thigh in a 53-year-old woman. (a, b) Coronal images through the thigh demonstrate an ovoid soft tissue mass (asterisk) that is hypointense to skeletal muscle on T1-weighted image (a) and markedly hyperintense on fast spin-echo T2-weighted fat-suppressed (FS) image (b). Myxoma lacks a true capsule, and a classic MR imaging feature of myxoma is irregular hyperintense signal (arrow) extending adjacent to the mass, due to infiltration of the tumor into the adjacent atrophic and edematous striated muscle. (c) Axial T1-weighted enhanced FS image shows the typical heterogeneous septal enhancement throughout the myxoma (arrow). (d) The myxoma was marginally resected, and gross specimen photograph shows a gelatinous mass with internal septae (asterisk).

T1-weighted imaging and hyperintense to fat on T2-weighted imaging. Lesions lack a feeding vessel, do not enhance, and insinuate between tissue planes (►Fig. 11b, c).^{39,53,60} Microcystic lesions may be intermediate in signal intensity on both T1- and T2-weighted images.⁵³

Chondro-Osseous Tumors

Soft tissue chondroma is the only benign chondro-osseous tumor classified by the WHO (►Fig. 11). Chondromas are painless tumors composed predominantly of hyaline cartilage that occur in extraosseous and extrasynovial locations.^{61,62} Nodules are almost always <3 cm, and most of the tumors occur in the fingers; however, lesions may also occur in the hands, toes, feet, trunk and head, and neck.^{61,62} Mineralization is invariably demonstrated on radiographs or CT, and masses are well circumscribed and approximate hyaline cartilage on all MRI sequences, except for signal voids at the site of mineralization (►Fig. 12).⁶³

Tumors of Uncertain Differentiation

Benign tumors of uncertain differentiation include lesions such as intramuscular myxoma and juxta-articular myxoma.⁶⁴ Intramuscular myxoma is a benign mesenchymal tumor characterized by abundant myxoid matrix, a small number of spindle-shaped cells, and a poorly developed vascular pattern.⁶⁵ Myxoma typically present as a painless palpable mass in the large muscles of the thigh, shoulder, buttocks, and upper arm in patients 40 to 70 years of age, more often in women.⁶⁵⁻⁶⁷ Tumors are most often solitary but may be multiple or coincide with fibrous dysplasia (Mazabraud syndrome).

On MRI, intramuscular myxoma is homogeneously low in signal intensity on T1-weighted MR sequences (►Fig. 13a), high signal intensity on T2-weighted or fluid-sensitive MR sequences (►Fig. 13b), and can have variable enhancement, most typically intense and heterogeneous (►Fig. 13c).⁶⁶⁻⁶⁸ Myxoma commonly has well-defined borders on MRI, although borders may be partially ill defined due to lack of a

true capsule and infiltration of the tumor into the adjacent atrophic and edematous striated muscle.^{66–68} A peritumoral fat rind can be present in 65% of cases, and increased signal in the adjacent muscle on fluid-sensitive sequences has been shown in 55%.⁶⁶ On gross examination, tumors are ovoid or globular and have a glistening gray-white or white appearance with stringy gelatinous contents with occasional small fluid-filled cystlike spaces (→**Fig. 12d**).⁶⁵ Local excision is curative.

Juxta-articular myxoma is rare and predominantly occurs around the knee. On MRI, this lesion is hypointense to skeletal muscle, hyperintense on T2-weighted imaging, and may involve the periarticular tendons, ligaments, joint capsule, muscles, and subcutaneous tissues.⁶⁹ Lesions may be differentiated from ganglia due to their fine internal structures and enhancement after contrast administration.⁶⁹

Neural Tumors

Although neural tumors are classified by the WHO under lesions of the nervous system, benign peripheral nerve sheath tumors are presented here because they are often included within the musculoskeletal and spine MRI examination field of view. Benign peripheral nerve sheath tumors are composed of neurilemoma (schwannoma) and neurofibroma, both of which contain cells closely related to the normal Schwann cell.⁷⁰ Neurilemoma is most often detected in patients between 20 and 50 years of age and represents 5% of all benign soft tissue tumors. Neurilemmomas most commonly occur in the cutaneous tissues of the head and neck, flexor surfaces of the extremities, posterior mediastinum, and retroperitoneum.⁷⁰ The neurilemoma is separable from the involved nerve, and surgical resection is curative. Neurilemmomas are solitary in the vast majority of cases but are plexiform or multiple in 5% of cases. Lesions occur with neurofibromatosis type 2 in 3% of cases.⁷⁰

Neurofibroma is most often detected in patients 20 to 30 years old and comprises >5% of all benign soft tissue tumors.^{70,71} The localized type of neurofibroma occurs in 90% of cases, with diffuse and plexiform types occurring less commonly. Neurilemoma and neurofibroma are difficult to differentiate on MRI, although some distinctive imaging features have been described. In fact, an estimated 70 to 90% of peripheral nerve sheath tumors have a diagnostic imaging appearance on MRI.¹ Both lesions can have a fusiform shape, although neurilemoma is more eccentric, and neurofibroma is centrally positioned relative to the nerve. Neurilemoma tends to be more heterogenous due to relative increases in the number of cystic cavitations, calcifications, and areas of central necrosis.^{72,73} Characteristic MR findings of the localized neurofibroma include low signal intensity on T1-weighted images, high signal intensity on T2-weighted imaging (→**Fig. 14**), and strong enhancement. Neurofibromas typically depict heterogeneously hyperintense signal on T2-weighted imaging, with low signal areas corresponding to fibrous and collagenous regions, and high signal areas corresponding to myxomatous stroma and cystic degeneration.

Both tumors can exhibit the “split-fat” and “target” signs. The “target sign” has been demonstrated in 58% of neuro-

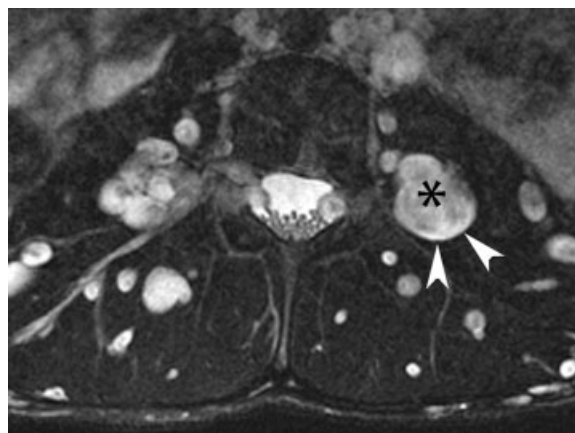


Fig. 14 Multiple neurofibromas in patient with neurofibromatosis. Axial fast spin-echo T2-weighted image through the lumbar spine shows multiple localized neurofibromas throughout the lumbar spine nerve roots, retroperitoneum, and paraspinous and psoas muscles. The “target sign” is evident in multiple tumors, with hypointense central collagenous/fibrotic component (asterisk) and peripheral myxomatous stroma (arrowheads).

fibromas and 15% of neurilemmomas on MRI, and it refers to the hypointense central area on T2-weighted imaging corresponding to fibrosis, with a more hyperintense myxomatous stroma in the margins of the tumor.⁷³ The “fat-split sign” is a peripheral brim of fat surrounding the lesion on T1-weighted imaging, corresponding to preservation of the normal fat around the neurovascular bundle.⁷³ Differentiating benign from malignant peripheral nerve sheath tumors (MPNSTs) on MRI is sometimes difficult, but worrisome features include large size (10 cm on average for MPNSTs versus 5 cm for neurofibroma), peripheral enhancement, perilesional edema-like signal changes, and intratumoral cystic lesions.⁷⁴

Conclusion

The vast majority of soft tissue tumors are benign and with a fairly definitive imaging diagnosis typically made in cases of lipoma, elastofibroma dorsi, hemangiomas, MO, and giant cell tumor of tendon sheath. In the remaining cases, the differential diagnosis can be narrowed by systematically assessing the patient’s age, anatomical location of the mass, clinical presentation, and any associated syndromes. It is very helpful to be aware of the WHO’s tumor designations and to be familiar with the incidence of specific tumors based on patient age, anatomical location, and characteristic MRI features.

References

- Murphey MD, Kransdorf MJ. Radiologic evaluation of soft tissue tumors. In: Weiss SW, Goldblum JR, eds. *Enzinger and Weiss’s Soft Tissue Tumors*. 5th ed. St. Louis, MO: Mosby; 2008:33–71
- Peterson JJ, Bancroft LW, Kransdorf MJ. Principles of tumor imaging. *Eur J Radiol* 2005;56(3):319–330
- Wu JS, Hochman MG. Soft-tissue tumors and tumorlike lesions: a systematic imaging approach. *Radiology* 2009;253(2):297–316

- 4 Stein-Wexler R. MR imaging of soft tissue masses in children. *Magn Reson Imaging Clin N Am* 2009;17(3):489–507, vi
- 5 Walker EA, Fenton ME, Salesky JS, Murphey MD. Magnetic resonance imaging of benign soft tissue neoplasms in adults. *Radiol Clin North Am* 2011;49(6):1197–1217, vi
- 6 Kransdorf MJ. Benign soft-tissue tumors in a large referral population: distribution of specific diagnoses by age, sex, and location. *AJR Am J Roentgenol* 1995;164(2):395–402
- 7 Bancroft LW, Peterson JJ, Kransdorf MJ, Berquist TH. Imaging of soft tissue lesions of the foot and ankle. *Radiol Clin North Am* 2008;46(6):1093–1103
- 8 Fletcher CDM, Unni JJ, Mertens F, eds. *World Health Organization Classification of Tumours: Tumours of Soft Tissue and Bone*. Lyon, France: IARC Press; 2000
- 9 Nielsen GP, Mandahi N. Lipoma. In: Fletcher CDM, Unni JJ, Mertens F, eds. *World Health Organization Classification of Tumours: Tumours of Soft Tissue and Bone*. Lyon, France: IARC Press; 2000:20–22
- 10 Bancroft LW, Kransdorf MJ, Peterson JJ, O'Connor MI. Benign fatty tumors: classification, clinical course, imaging appearance, and treatment. *Skeletal Radiol* 2006;35(10):719–733
- 11 Bancroft LW, Kransdorf MJ, Peterson JJ, Sundaram M, Murphey MD, O'Connor MI. Imaging characteristics of spindle cell lipoma. *AJR Am J Roentgenol* 2003;181(5):1251–1254
- 12 Kransdorf MJ, Bancroft LW, Peterson JJ, Murphey MD, Foster WC, Temple HT. Imaging of fatty tumors: distinction of lipoma and well-differentiated liposarcoma. *Radiology* 2002;224(1):99–104
- 13 Ha TV, Kleinman PK, Fraire A, et al. MR imaging of benign fatty tumors in children: report of four cases and review of the literature. *Skeletal Radiol* 1994;23(5):361–367
- 14 Sciot R, Mandahl N. Lipoblastoma/lipoblastomatosis. In: Fletcher CDM, Unni JJ, Mertens F, eds. *World Health Organization Classification of Tumours: Tumours of Soft Tissue and Bone*. Lyon, France: IARC Press; 2000:26–27
- 15 Chen CW, Chang WC, Lee HS, Ko KH, Chang CC, Huang GS. MRI features of lipoblastoma: differentiating from other palpable lipomatous tumor in pediatric patients. *Clin Imaging* 2010;34(6):453–457
- 16 Weiss SW, Goldblum JR. Benign lipomatous tumors. In: Weiss SW, Goldblum JR, eds. *Enzinger and Weiss's Soft Tissue Tumors*. 5th ed. St. Louis, MO: Mosby; 2008:429–476
- 17 Nielsen GP, Rosenberg AE. Lipomatosis. In: Fletcher CDM, Unni JJ, Mertens F, eds. *World Health Organization Classification of Tumours: Tumours of Soft Tissue and Bone*. Lyon, France: IARC Press; 2000:23–24
- 18 McEachern A, Janzen DL, O'Connell JX. Shoulder girdle lipomatosis. *Skeletal Radiol* 1995;24(6):471–473
- 19 Gutzeit A, Binkert CA, Schmidt S, et al. Growing fatty mass in the back: diagnosis of a multiple symmetric lipomatosis (Madelung's disease) in association with chronic alcoholism. *Skeletal Radiol* 2012;41(4):465–466; 489–490
- 20 Robbin MR, Murphey MD, Temple HT, Kransdorf MJ, Choi JJ. Imaging of musculoskeletal fibromatosis. *Radiographics* 2001;21(3):585–600
- 21 Lee JC, Thomas JM, Phillips S, Fisher C, Moskovic E. Aggressive fibromatosis: MRI features with pathologic correlation. *AJR Am J Roentgenol* 2006;186(1):247–254
- 22 Weiss SW, Goldblum JR. Fibromatoses. In: Weiss SW, Goldblum JR, eds. *Enzinger and Weiss's Soft Tissue Tumors*. 5th ed. St. Louis, MO: Mosby; 2008:227–256
- 23 Goldblum JR, Fletcher JA. Desmoid-type fibromatoses. In: Fletcher CDM, Unni JJ, Mertens F, eds. *World Health Organization Classification of Tumours: Tumours of Soft Tissue and Bone*. Lyon, France: IARC Press; 2000:83–84
- 24 Oweis Y, Lucas DR, Brandon CJ, Girish G, Jacobson JA, Fessell DP. Extra-abdominal desmoid tumor with osseous involvement. *Skeletal Radiol* 2012;41(4):483–487
- 25 Kransdorf MJ, Murphey MD. Benign fibrous and fibrohistiocytic tumors. In: Kransdorf MJ, Murphey MD, ed. *Imaging of Soft Tissue Tumors*. 2nd ed. Philadelphia, PA: Lippincott Williams & Wilkins; 2006:189–256
- 26 Kransdorf MJ, Jelinek JS, Moser RP Jr, et al. Magnetic resonance appearance of fibromatosis. A report of 14 cases and review of the literature. *Skeletal Radiol* 1990;19(7):495–499
- 27 McCarville MB, Hoffer FA, Adelman CS, Khoury JD, Li C, Skapek SX. MRI and biologic behavior of desmoid tumors in children. *AJR Am J Roentgenol* 2007;189(3):633–640
- 28 Dinauer PA, Brixey CJ, Moncur JT, Fanburg-Smith JC, Murphey MD. Pathologic and MR imaging features of benign fibrous soft-tissue tumors in adults. *Radiographics* 2007;27(1):173–187
- 29 Hashimoto H, Bridge JA. Elastofibroma. In: Fletcher CDM, Unni JJ, Mertens F, eds. *World Health Organization Classification of Tumours: Tumours of Soft Tissue and Bone*. Lyon, France: IARC Press; 2000:56–57
- 30 Tamimi Mariño I, Sesma Solis P, Pérez Lara A, Martínez Malo J, Vazquez ML, Tamimi F. Sensitivity and positive predictive value of magnetic resonance imaging in the diagnosis of elastofibroma dorsi: review of fourteen cases. *J Shoulder Elbow Surg* 2013;22(1):57–63
- 31 Naylor MF, Nascimento AG, Sherrick AD, McLeod RA. Elastofibroma dorsi: radiologic findings in 12 patients. *AJR Am J Roentgenol* 1996;167(3):683–687
- 32 Rosenberg AE. Myositis ossificans and fibroosseous pseudotumor of digits. In: Fletcher CDM, Unni JJ, Mertens F, eds. *World Health Organization Classification of Tumours: Tumours of Soft Tissue and Bone*. Lyon, France: IARC Press; 2000:52–54
- 33 Tyler P, Saifuddin A. The imaging of myositis ossificans. *Semin Musculoskelet Radiol* 2010;14(2):201–216
- 34 Blankenbaker DG, Tuite MJ. Temporal changes of muscle injury. *Semin Musculoskelet Radiol* 2010;14(2):176–193
- 35 Shelly MJ, Hodnett PA, MacMahon PJ, Moynagh MR, Kavanagh EC, Eustace SJ. MR imaging of muscle injury. *Magn Reson Imaging Clin N Am* 2009;17(4):757–773; vii
- 36 De St Aubain Somerhausen N, Dal Cin P. Giant cell tumour of tendon sheath. In: Fletcher CDM, Unni JJ, Mertens F, eds. *World Health Organization Classification of Tumours: Tumours of Soft Tissue and Bone*. Lyon, France: IARC Press; 2000:110–111
- 37 Fox MG, Kransdorf MJ, Bancroft LW, Peterson JJ, Flemming DJ. MR imaging of fibroma of the tendon sheath. *AJR Am J Roentgenol* 2003;180(5):1449–1453
- 38 Hashimoto H, Quade B. Angioleiomyoma. In: Fletcher CDM, Unni JJ, Mertens F, eds. *World Health Organization Classification of Tumours: Tumours of Soft Tissue and Bone*. Lyon, France: IARC Press; 2000:128–129
- 39 Davies CE, Davies AM, Kindblom LG, James SL. Soft tissue tumors with muscle differentiation. *Semin Musculoskelet Radiol* 2010;14(2):245–256
- 40 Ogura K, Goto T, Nemoto T. Painless giant angioleiomyoma in the subfascia of the lower leg. *J Foot Ankle Surg* 2012;51(1):99–102
- 41 Jalgaonkar A, Dachehalli S, Farid M, Rao S. Angioleiomyoma of the knee: case series and an unusual cause of knee pain. *J Knee Surg* 2011;24(1):33–37
- 42 Gupte C, Butt SH, Tirabosco R, Saifuddin A. Angioleiomyoma: magnetic resonance imaging features in ten cases. *Skeletal Radiol* 2008;37(11):1003–1009
- 43 Hashimoto H, Quade B. Leiomyoma of deep soft tissue. In: Fletcher CDM, Unni JJ, Mertens F, eds. *World Health Organization Classification of Tumours: Tumours of Soft Tissue and Bone*. Lyon, France: IARC Press; 2000:130
- 44 Miki Y, Abe S, Tokizaki T, Harasawa A, Imamura T, Matsushita T. Imaging characteristics of calcified leiomyoma of deep soft tissue. *J Orthop Sci* 2007;12(6):601–605
- 45 Jalgaonkar A, Mohan A, Dawson-Bowling S, Skinner J, Briggs TW. Deep soft tissue leiomyoma mimicking fibromatosis in a 5-year-old male. *J Foot Ankle Surg* 2012;51(1):110–113

- 46 Folpe AL. Glomus tumours. In: Fletcher CDM, Unni JJ, Mertens F, eds. *World Health Organization Classification of Tumours: Tumours of Soft Tissue and Bone*. Lyon, France: IARC Press; 2000:110–111
- 47 Glazebrook KN, Laundre BJ, Schiefer TK, Inwards CY. Imaging features of glomus tumors. *Skeletal Radiol* 2011;40(7):855–862
- 48 Kransdorf MJ, Murphey MD. Vascular and lymphatic tumors. In: Kransdorf MJ, Murphey MD, eds. *Imaging of Soft Tissue Tumors*. 2nd ed. Philadelphia, PA: Lippincott Williams & Wilkins; 2006:150–188
- 49 Kapadia SB, Barr FG. Rhabdomyoma. In: Fletcher CDM, Unni JJ, Mertens F, eds. *World Health Organization Classification of Tumours: Tumours of Soft Tissue and Bone*. Lyon, France: IARC Press; 2000:142–145
- 50 Weiss SW, Goldblum JR. Rhabdomyoma. In: Weiss SW, Goldblum JR, eds. *Enzinger and Weiss's Soft Tissue Tumors*. 5th ed. St. Louis, MO: Mosby; 2008:583–594
- 51 Kransdorf MJ, Murphey MD, et al. Muscle tumors. In: Kransdorf MJ, Murphey MD, eds. *Imaging of Soft Tissue Tumors*. 2nd ed. Philadelphia, PA: Lippincott Williams & Wilkins; 2006:298–327
- 52 Calonje E. Hemangiomas. In: Fletcher CDM, Unni JJ, Mertens F, eds. *World Health Organization Classification of Tumours: Tumours of Soft Tissue and Bone*. Lyon, France: IARC Press; 2000:156–158
- 53 Cahill AM, Nijs EL. Pediatric vascular malformations: pathophysiology, diagnosis, and the role of interventional radiology. *Cardiovasc Intervent Radiol* 2011;34(4):691–704
- 54 Weiss SW, Goldblum JR. Benign tumors and tumor-like lesions of blood vessels. In: Weiss SW, Goldblum JR, eds. *Enzinger and Weiss's Soft Tissue Tumors*. 5th ed. St. Louis, MO: Mosby; 2008:633–679
- 55 Kramer U, Ernemann U, Fenchel M, et al. Pretreatment evaluation of peripheral vascular malformations using low-dose contrast-enhanced time-resolved 3D MR angiography: initial results in 22 patients. *AJR Am J Roentgenol* 2011;196(3):702–711
- 56 Elsayes KM, Menias CO, Dillman JR, Platt JF, Willatt JM, Heiken JP. Vascular malformation and hemangiomas syndromes: spectrum of imaging manifestations. *AJR Am J Roentgenol* 2008;190(5):1291–1299
- 57 Mertens F, Unni K. Enchondromatosis: Ollier disease and Maffucci syndrome. In: Fletcher CDM, Unni JJ, Mertens F, eds. *World Health Organization Classification of Tumours: Tumours of Soft Tissue and Bone*. Lyon, France: IARC Press; 2000:356–357
- 58 Beham A. Lymphangioma. In: Fletcher CDM, Unni JJ, Mertens F, eds. *World Health Organization Classification of Tumours: Tumours of Soft Tissue and Bone*. Lyon, France: IARC Press; 2000:162–163
- 59 Ly JQ, Gilbert BC, Davis SW, Beall DP, Richardson RR. Lymphangioma of the foot. *AJR Am J Roentgenol* 2005;184(1):205–206
- 60 Kransdorf MJ, Murphey MD. Vascular and lymphatic tumors. In: Kransdorf MJ, Murphey MD, eds. *Imaging of Soft Tissue Tumors*. 2nd ed. Philadelphia, PA: Lippincott Williams & Wilkins; 2006:150–188
- 61 Naylor S, Heim S. Soft tissue chondroma. In: Fletcher CDM, Unni JJ, Mertens F, eds. *World Health Organization Classification of Tumours: Tumours of Soft Tissue and Bone*. Lyon, France: IARC Press; 2000:180–181
- 62 Weiss SW, Goldblum JR. Cartilaginous soft tissue tumors. In: Weiss SW, Goldblum JR, eds. *Enzinger and Weiss's Soft Tissue Tumors*. 5th ed. St. Louis, MO: Mosby; 2008:1017–1038
- 63 Kransdorf MJ, Murphey MD. Extraskelletal osseous and cartilaginous tumors. In: Kransdorf MJ, Murphey MD, eds. *Imaging of Soft Tissue Tumors*. 2nd ed. Philadelphia, PA: Lippincott Williams & Wilkins; 2006:427–480
- 64 Nielsen GP, Steinman G. . Intramuscular myxoma. In: Fletcher CDM, Unni JJ, Mertens F, eds. *World Health Organization Classification of Tumours: Tumours of Soft Tissue and Bone*. Lyon, France: IARC Press; 2000:186–187
- 65 Weiss SW, Goldblum JR. Benign soft tissue tumors and pseudotumors of uncertain type. In: Weiss SW, Goldblum JR, eds. *Enzinger and Weiss's Soft Tissue Tumors*. 5th ed. St. Louis, MO: Mosby; 2008:1063–1092
- 66 Bancroft LW, Kransdorf MJ, Menke DM, O'Connor MI, Foster WC. Intramuscular myxoma: characteristic MR imaging features. *AJR Am J Roentgenol* 2002;178(5):1255–1259
- 67 Murphey MD, McRae GA, Fanburg-Smith JC, Temple HT, Levine AM, Abouafia AJ. Imaging of soft-tissue myxoma with emphasis on CT and MR and comparison of radiologic and pathologic findings. *Radiology* 2002;225(1):215–224
- 68 Kransdorf MJ, Murphey MD. Tumors of uncertain histogenesis. In: Kransdorf MJ, Murphey MD, eds. *Imaging of Soft Tissue Tumors*. 2nd ed. Philadelphia, PA: Lippincott Williams & Wilkins; 2006:481–510
- 69 Somford MP, de Vries JS, Dingemans W, et al. Juxta-articular myxoma of the knee. *J Knee Surg* 2011;24(4):299–301
- 70 Kransdorf MJ, Murphey MD. Neurogenic tumors. In: Kransdorf MJ, Murphey MD, eds. *Imaging of Soft Tissue Tumors*. 2nd ed. Philadelphia, PA: Lippincott Williams & Wilkins; 2006:328–380
- 71 Weiss SW, Goldblum JR. Benign tumors of peripheral nerves. In: Weiss SW, Goldblum JR, eds. *Enzinger and Weiss's Soft Tissue Tumors*. 5th ed. St. Louis, MO: Mosby; 2008:903–944
- 72 Abreu EAS, Aubert S, Wavreille G, Gheno R, Canella C, Cotten A. Peripheral tumor and tumor-like neurogenic lesions. *Eur J Radiol* 2013;82(1):38–50
- 73 Jee WH, Oh SN, McCauley T, et al. Extraaxial neurofibromas versus neurilemmomas: discrimination with MRI. *AJR Am J Roentgenol* 2004;183(3):629–633
- 74 Wasa J, Nishida Y, Tsukushi S, et al. MRI features in the differentiation of malignant peripheral nerve sheath tumors and neurofibromas. *AJR Am J Roentgenol* 2010;194(6):1568–1574